Chemical composition of ferrierite

WILLIAM S. WISE

Department of Geological Sciences, University of California
Santa Barbara, California 93106

AND R. W. TSCHERNICH

532 Avenue A, Snohomish, Washington 98920

Abstract

Ferrierite specimens from localities at Altoona, Washington; Silver Mountain, Alpine County, California; and Pinaus Lake, Monte Lake, and Francois Lake, British Columbia, have been analyzed by microprobe methods. These new analyses are combined with available data to delineate the compositional range for this zeolite.

The frame work composition ranges from $(Al_{7.5}Si_{27.5}O_{72})$ to $(Al_5Si_{31}O_{72})$. The *a* cell dimension varies linearly with the Si content. There are between 3 and 5 exchangeable cations (univalent and divalent) per unit cell of 72 oxygens, but with wide variations; the amount of univalent ions ranges from 21 to 85 percent. There is no clear parititioning of the univalent ions, as the $Na/(Na+K)$ ratio is highly variable. Mg is clearly fractionated in all ferrierites $(Ca/(Ca+Mg) < 0.40)$, regardless of the amount of divalent ions. The highest known amounts of BaO (2.54%) and SrO (0.40%) are in the Silver Mountain ferrierite.

Associated zeolites commonly include clinoptilolite or heulandite, although mordenite and dachiardite also occur with ferrierite at Altoona.

The broad compositional range of ferrierite indicates that it can crystallize from solutions with a wide variety of alkali and alkaline earth cations, none of which are essential to the zeolite. If present, Mg ions are fractionated into the zeolite. Ferrierite crystallizes in response to high silica activities. However, to account for the range in silica contents, the a_{SiO_2} must be coupled with other variables, such as temperature or a_{H_2O}, in order to prevent crystallization of other high silica zeolites.

Introduction

There have been few published analyses of the zeolite ferrierite, even though it is now known to be more common than once believed, occurring both as a cavity-filling material in basaltic rocks and as a diagenetic mineral in rhyolite tuffaceous sediments. Following the original description of ferrierite from Kamloops Lake, British Columbia, by Graham (1918), it was not until 1967 that another occurrence was discovered and described by Alietta, Passaglia, and Scaini (1967). Then ferrierite was analyzed and described from two localities in California (Wise, Nokleberg, and Kokinos, 1969), one in Japan (Yajima, Nakamura, and Ishii, 1971), and Austria (Zirkl, 1973). Regis (1970) reported the existence and composition of ferrierite forming extensive beds in central Nevada.

Ferrierite from five more localities in the western United States and Canada has now been collected and analyzed. The purpose of this paper is to present this new analytical data, which illustrates a broad range of compositional variation, and to show the chemical relationships with closely associated zeolites.

Ferrierite is a silica-rich zeolite, forming thin, bladed crystals of orthorhombic symmetry. The crystal structure, determined by Vaughan (1966), is characterized by $(Si,Al)O_4$ tetrahedra forming five-member rings linked in complex chains parallel to the orthorhombic *c* axis. Between the chains in each unit cell are two large cation cages, which contain hydrated cations, commonly Mg^{2+}, and two channels, containing the loosely bound and highly disordered remaining cations and water molecules.

Sample locations

Altoona, Washington

Ferrierite occurs in the Miocene Columbia River basalts near Altoona in western Wahkiakum County, southwestern Washington. The zeolite-bearing rock originally came from a small quarry near the east end of the settlement of Altoona, but most of the specimens were collected from riprap along the Columbia River in Altoona and an area about one mile west of the town.

The ferrierite occurs as linings and radial groups of white or colorless blades in small vesicles and open spaces between fragments of brecciated basalt. The basalt consists of abundant glass with less than 20 percent plagioclase and clinopyroxene. Some fragments contain vesicles (1 cm) commonly lined with siderite and covered with greenish-black nontronitic clay.

The habit and forms of the ferrierite are nearly identical with that from Agoura in the Santa Monica Mountains, California (Wise *et al*, 1969). In both areas crystals display a dominant (010) face, while those from British Columbia have a dominant (100) face. Closely associated with ferrierite at Altoona is Ca-clinoptilolite, dachiardite, mordenite, chalcedony, and calcite—all have grown on the siderite and clay lining. A common sequence of crystallization is siderite, clay, mordenite, ferrierite, and Ca-clinoptilolite, followed by dachiardite. A detailed description of these minerals is in preparation.

Kamloops Lake, British Columbia

The type area for ferrierite, first described by Graham (1918), is in a cut along the Canadian Northern Railway on the north shore of Kamloops Lake, east of Kamloops, southern British Columbia. Even though this ferrierite has been adequately described, it was recollected along with the associated clinoptilolite for more complete analysis. The zeolites occur in a deeply weathered, porphyritic olivine-basalt flow-breccia in the Kamloops Group of middle Tertiary age (Cockfield, 1947).

Ferrierite has formed in seams and vesicles in the flow-breccia. Within them calcite and chalcedony may cover the earlier-formed ferrierite. Pale brownish-red clinoptilolite is sparsely associated with the ferrierite, which occurs as colorless to red stained blades, forming linings and radiating balls up to 15 mm in diameter.

Monte Lake, British Columbia

Ferrierite has been found near Monte Lake, about 6 miles west of Westwold along Highway 97W, southeastern Kamloops District, British Columbia, in basalt flows belonging to the middle Tertiary Kamloops Group (see Jones, 1959). The ferrierite occurs lining vesicles and in calcite-filled nodules in a fine-grained, greenish-black basalt composed of microphenocrysts of labradorite and augite set in an opaque glass matrix in a large roadcut east of Monte Lake and along railway cuts one mile south of the lake. Ferrierite also occurs in basalts, exposed by logging roads south of Monte Lake.

The ferrierite occurs as colorless to salmon-colored, thin blades which range from 5 to 15 mm long. In the past this material has been mis-identified as either mordenite or mesolite, probably because of the thinness of the crystals. Other minerals include analcime, chabazite, heulandite, levyne, stilbite, and thomsonite.

Pinaus Lake, British Columbia

Ferrierite has recently been found in altered basalts of the Kamloops Group along the shore of Pinaus Lake, 8 miles southeast of Westwold, British Columbia (see Jones, 1969). This occurrence is similar to the Kamloops Lake location, in that the ferrierite is found as cavity linings of calcite-filled nodules. The crystals are short, red to white blades, which are commonly arranged in orderly rows of crystals crossing each ball of crystals.

Francois Lake, British Columbia

The late R. M. Thomson found ferrierite as minute needles on collinsite and carbonate-fluorapatite at Francois Lake, over 300 miles northwest of Kamloops Lake. In the same rocks, ferrierite is also found apart from the phosphates in breccia cavities and vesicles of the brown, aphyric andesitic rocks of Tertiary age in that area. This latter ferrierite occurs as small (2 mm) colorless blades and radial groups associated with 1 mm crystals of brownish heulandite.

Silver Mountain, California

In altered andesite near the old townsite of Silver Mountain, southwest of Markleeville in Alpine County, California, ferrierite occurs as very thin, white to orange blades. These commonly form mats of crystals but also combine to form compact balls and short rows of oriented crystals, similar to that found at Pinaus Lake, British Columbia. Ferrierite is associated with sparse heulandite and barite.

Rodope Mountains, Bulgaria

A container of ferrierite crystals labelled "Rodope Mountains, Bulgaria," was included in a suite of

zeolite specimens sent to us from Drs. Golubova and Belitsky of the Siberian Branch of the Academy of Sciences of the U.S.S.R.

Electron microprobe and X-ray data

All of the ferrierite samples analyzed here are clusters of very small blades; some are less than 10 micrometers in thickness. Therefore, whole clusters were embedded in epoxy, and ground until the center of the cluster was exposed. The mount was then polished and coated with 250 A of carbon. The analyses were made on an ARL electron microprobe, using an accelerating voltage of 15 kilovolts for all elements with a sample current of 10 nanoamps. Standards

TABLE 1.   Analyses of Ferrierites

	1	2	3	4	5	6	7	8	9
Locality	Altoona[†] Wash.	Altoona[†] Wash.	Sta. Monica Mtns., Cal.	Kamloops Lake, B.C.	Pinaus Lake, B.C.	Francois Lake, B.C.	Monte Lake B.C.	Silver Mtn. Cal.	Rodope Mtns. Bulgaria
n*	2	2	8	4	6	4	2	2	3
SiO_2	71.50	72.18	73.07	70.14	67.79	66.11	66.33	65.02	70.00
Al_2O_3	10.18	10.87	10.00	11.45	11.00	13.20	13.18	13.19	11.31
Fe_2O_3	0.01	0.05	0.02	0.13	1.57	0.30	0.27	0.12	(0.30)
MgO	0.59	1.52	1.19	2.56	3.23	3.34	3.41	3.00	2.15
CaO	0.11	0.97	0.30	0.15	0.51	1.02	1.39	1.05	1.62
SrO	0.13	0.0	0.0	0.18	0.0	0.0	0.34	0.40	0.71
BaO	0.13	0.38	0.09	0.38	0.88	1.97	0.41	2.54	0.25
Na_2O	3.64	1.53	1.38	1.86	0.44	0.41	0.50	0.21	0.31
K_2O	1.73	1.54	3.78	0.63	1.46	0.83	1.17	1.48	0.75
Total **	88.02	89.43	89.83	87.48	86.88	87.28	87.00	87.01	87.40
Cell contents based on 72 oxygens									
Si	30.86	30.62	31.01	30.22	29.78	29.06	29.05	28.99	30.32
Al	5.15	5.43	5.00	5.81	5.69	6.89	6.80	6.93	5.77
Fe	--	--	--	.04	.52	.10	.09	.04	--
Mg	.38	.96	.74	1.64	2.12	2.19	2.23	1.99	1.39
Ca	.05	.44	.14	.07	.24	.48	.65	.50	.75
Sr	.03	--	--	.04	--	--	.09	.10	.18
Ba	.02	.06	--	.07	.15	.34	.07	.45	.04
Na	3.06	1.26	1.14	1.55	.37	.35	.43	.18	.26
K	.97	1.05	2.05	.35	.82	.46	.65	.84	.42
Si+Al+Fe	36.01	36.05	36.01	36.07	35.99	36.05	35.94	35.96	36.09
Σch	5.00	5.24	4.95	5.54	6.24	6.83	7.16	7.10	5.40
Error	+3.0%	+3.6%	+1.0%	+5.6%	−0.5%	+2.3%	−3.8%	−1.8%	+6.9%
Refractive Indices									
α	1.473	1.474	1.477	1.479	--	--	--	--	--
β	1.474	--	--	1.480	1.482	1.482	1.482	1.483	1.481
γ	1.477	1.478	1.480	1.483	1.484	1.485	1.485	1.486	1.484
Refined Cell Dimensions [††]									
a_o	18.90(1)	19.05(1)	18.973(7)	19.164(8)	19.205(4)	19.218(5)	19.222(7)	19.224(3)	19.161(4)
b_o	14.141(7)	--	14.140(6)	14.151(5)	14.151(5)	14.153(5)	14.147(7)	14.142(4)	14.156(5)
c_o	7.487(7)	--	7.478(4)	7.496(3)	7.496(3)	7.509(3)	7.54(1)	7.510(2)	7.500(3)

* Number of analyses averaged from each locality; all analyses are plotted on figures 1 and 3.

† Two different habits of ferrierite: col. 1 - diamond-shape (010) with (100) and (201); col. 2: typical bladed habit (010) with (100) and (001) terminations.

†† Parenthesized figures represent the estimated standard deviation (esd) in terms of least units cited for the value to their immediate left, thus 18.90(1) indicates an esd of 0.01.

** The remainder is the H_2O; the amount is not a good measure of the H_2O content, since some is lost in the vacuum.

used are scolecite (Ca and Al), K-feldspar (K and Si), albite (Na), olivine (Mg), hematite (Fe), sanbornite (Ba), and celestite (Sr). Emission data were reduced with a modified version of EMPADR 7 (Rutlidge and Gasparrini, 1969, Department of Geology, University of Toronto).

Analysis of zeolite minerals with the electron microprobe encounters several difficulties, which can degrade the final results. The beam heats the sample causing partial volatilization and loss of the weakly bonded water, which causes bubbling of the carbon coating. During the water loss there is a small increase in the counting rates of the abundant elements like Si and Al. Sodium ions, weakly bonded in channels, are probably driven into the sample by the electron beam, causing sharp drops in counting rates. In addition, the low density zeolite structure allows deep penetration of the electrons. Small crystals (about 5 micrometers) invariably give low totals, indicating the excitation volume includes more than the zeolite crystal. In order to overcome these problems at least partially, spot sizes as large as possible were used (up to 20 micrometers, if the sample size permitted). The spot was moved after every 10-second counting period, especially when analyzing for alkali metals, and only the largest crystals were analyzed.

Since zeolite minerals are framework silicates with alkali and alkaline earth ions balancing the charge imbalance caused by aluminum substitution for silicon, there are two sensitive internal checks on the quality of the analysis. For ferrierite, the Al + Si must total 36 in the unit cell of 72 oxygens, and the sum of the charges of the alkali and alkaline earth ions (exchangeable ions) must equal the number of tetrahedral Al. Excess Al is almost certainly a result of analytical error and should not be considered a component of the exchangeable ions.

The analyses (Table 1) can be evaluated by the value of an error function $E = [(Al+Fe^{3+})^{IV} - \Sigma$ charge/Σ charge] $\times$ 100, where Σ charge is the sum of the charges of the exchangeable ions (*cf* Passaglio, 1970, p. 1279). A balancing error greater than ± 7 percent is taken as indicating unreliable analytical results.

X-ray powder diffraction data were obtained on each of the analyzed samples. Unit cell dimensions were refined from X-ray diffraction powder data, using the U. S. Geological Survey's FORTRAN IV computer program W7214, and are reported in Table 1. The peaks used in the refinements are those listed in Wise *et al* (1969, Table 4). The smallest errors were obtained on samples with the smallest range of compositions.

Discussion of results

All available analyses of ferrierite have been plotted on Figure 1 to show the relative abundances of Si, divalent, and univalent ions. In a unit cell of 72 oxygens where Si + Al very nearly equals 36, Si ranges from 27.5 to 31.0, corresponding to Si/Al ratios of 3.2 to 6.2, respectively. This variation and range of Si contents is similar to those of other high-Si zeolites, such as the chabazite and the heulandite groups, except that ferrierite reaches higher Si contents. It is interesting to note that many ferrierites which crystallized in cavities of basalts reach higher Si contents than do those which formed from rhyolite glass (points F and L, Fig. 1).

Comparison of the chemical data and cell dimensions in Table 1 reveals a strong linear relationship between the *a*-cell dimension and the Si content. Figure 2 is a plot of these two parameters. Causes for departure from a straight line may result in part from inaccuracies in the chemical composition determination. However, the wide departure of the Altoona #1 point must have some other cause. The correlation is sufficiently good that approximate compositions of the ferrierite can be obtained from an X-ray pattern.

Figure 1 illustrates that the univalent to divalent substitution can vary from 85 percent Na+K ions (Altoona, Table 1, col. 1), to about 21 percent Na+K ions (Francois Lake ferrierite, col. 6) without large accompanying changes in Si content. The distribution of points in Figure 1 also demonstrates that the ferrierites with the lower Si contents are accompanied by a predominance of divalent cations. The reason for this is not clear, since it cannot be entirely related to site availability. In refining the crystal structure of ferrierite, Vaughan (1966) was able to locate two specific cation locations and two channels with room for only two more fully hydrated cations. The total number of cations in the ferrierites in Table 1 and others from the literature (see Fig. 1 for references) varies from 3 to nearly 5. The excess over four are apparently accommodated by partial hydration and random occurrence within the channels.

Relative concentrations of the four major cation species occupying exchangeable ion sites are plotted in Figure 3. All the ferrierites from basaltic rocks show a distinct preference for Mg over Ca, regardless of the total amount of these ions. Ferrierite synthesized from K-Na solutions (Cormier and Sand, in preparation) strongly fractionated the K relative to the composition of the solution. The wide spread of Na/(Na+K) ratios indicates either no strong parti-
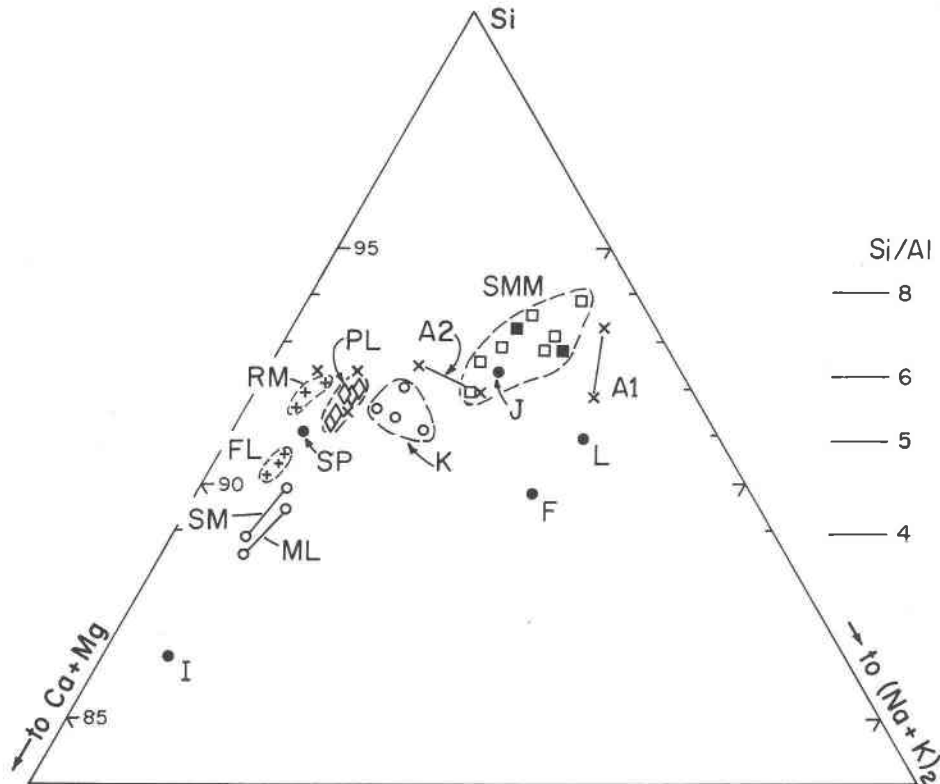
FIG. 1. Si–Ca+Mg–(Na+K)$_2$ plot of all analyzed ferrierites. Solid symbols represent published analyses; all others, analyses from this work. Points connected by lines represent compositions from a single crystal; multiple points from one locality have been averaged for inclusion in Table 1. Symbols: all X's, A-1, and A-2 Altoona, Washington (cols. 1 and 2, Table 1); SMM—squares, Santa Monica Mountains (Agoura, Wise *et al,* 1969); PL—Pinaus Lake, B.C.; RM—Rodope Mountains, Bulgaria; FL—Francois Lake, B. C.; K—Kamloops Lake, B. C.; J—Japan (Yajima *et al,* 1973); SP—Sonora Pass, California (Wise *et al,* 1969); I—Italy (Alietta *et al,* 1967); and L—Lovelock, F—Fallon, Nevada (Regis, 1970).
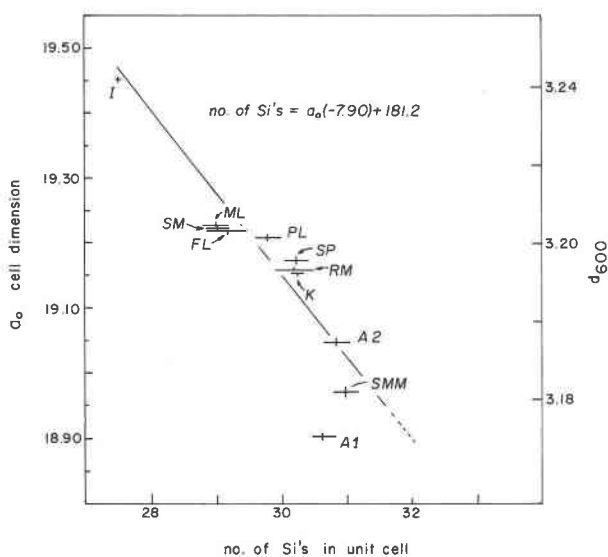
FIG. 2. Plot of a_0 cell dimensions *vs* number of Si ions per unit cell. Locality symbols are the same as in Figure 1. Linear regression includes all points but A-1, yielding R = −0.95.

tioning from natural waters, or that these waters have very low a_{K+}.

Most of the zeolites analyzed in this study reveal some compositional difference between the cores or bases of crystals to the outermost extremities (see, for example, the PL points in Fig. 3). The changing composition of the solution as the zeolite is growing has little effect on the Si/Al content (*cf* Fig. 1), but is reflected in the exchangeable ions.

Ba and Sr are present in many of the ferrierites but in small quantities. The highest amounts are in the Silver Mountain material, where the ferrierite is associated with barite.

Associated zeolites

Like most other zeolites, ferrierite crystallization is preceded by clay, which raises the pH in the pore solutions, to give the necessary high silica activites. In order to determine the relative activity levels that cause the formation of ferrierite, it is necessary to
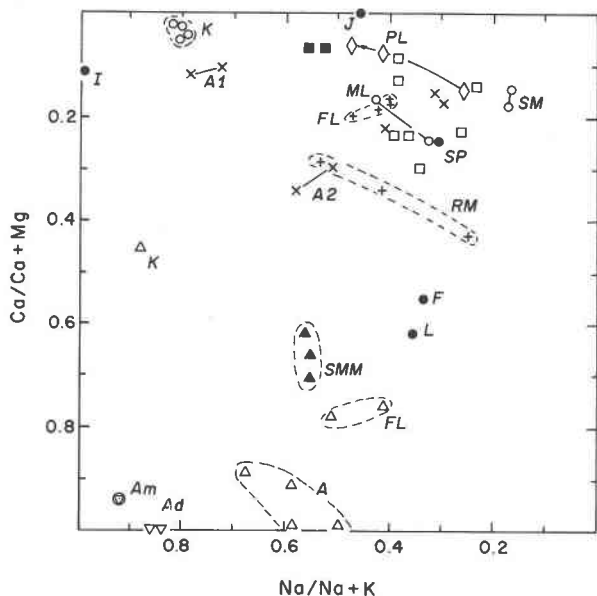
FIG. 3. Plot of Ca/(Ca+Mg) *vs* Na/(Na+K) for all ferrierites of Figure 1, as well as all analyzed associated minerals. Symbols are the same as Figure 1. Triangles represent clinoptilolite and heulandite (Table 3); inverted triangles, Ad—dachiardite and Am—mordenite from Altoona, Washington. Note that all ferrierites, except F and L, have Ca/(Ca+Mg) < 0.4, and that the associated clinoptilolite and heulandites have slightly higher Na/(Na+K) ratios than the ferrierites.

examine the composition of the closely associated zeolite phases. Clinoptilolite (or heulandite) occurs most commonly with ferrierite, but at Altoona the assemblage also includes mordenite and dachiardite. As in most assemblages of zeolites from amygdules, it is difficult to demonstrate that these minerals co-existed in equilibrium, because they generally grow sequentially. In addition, they rarely grow at the expense of an earlier phase.

Table 2 contains microprobe analyses of zeolites associated with the ferrierites in Table 1. These data have been plotted on Figures 3 and 4, and provide evidence for the conclusion that specific cation activities have significantly less control over which of the two zeolitic frameworks crystallize than does the activity of silica.

The Na/(Na+K) ratios of zeolites from the same localities are nearly the same, but the Ca/(Ca+Mg) ratios are markedly different (Fig. 3). Clinoptilolite and heulandite apparently do not have cation positions especially suited to any particular cation, since they occur along the sides of channels (Merkle and Slaughter, 1968). However, the cation cages in ferrierite are particularly suited for hydrated Mg cations, which are selectively removed from the solu-

tion by the zeolite. Because the ferrierites from the Santa Monica Mountains and Altoona contain 0.25 (Wise *et al*, 1969) and 0.38 Mg ions, respectively, this is apparently not required for the formation of the framework.

The variety of tie line slopes in Figure 4 indicates that neither the ferrierite nor the clinoptilolite phases have a preference for cations of particular charge. These different divalent/univalent ratios are probably related to changes in the solution chemistry as the earlier phase crystallizes.

The clinoptilolites or heulandites associated with ferrierite are less siliceous (Fig. 4) and by roughly the same amount (about one Si per unit cell of 72 oxygens), regardless of the total exchangeable cation content. If crystallization of the ferrierite takes place in response to a certain a_{SiO_2} in the solution, the clinoptilolite apparently crystallizes in response to a lower a_{SiO_2}, because the two zeolites do not grow simultaneously. The boundary value of a_{SiO_2} is clearly not the same at each locality, because the Si content of the Santa Monica Mountain clinoptilolite is greater than that of the Francois Lake ferrierite. The a_{SiO_2} can be lowered by increases in temperature or some other variable, such as the salinity (a_{H_2O}).

TABLE 2. Analyses of Minerals Associated with Ferrierite

mineral locality	heulandite Francois Lake, B.C.	clinoptilolite Kamloops Lake B.C.	clinoptilolite Altoona, Wash.	clinoptilolite* Sta. Monica Mtns. California
SiO_2	60.32	64.58	65.01	69.93
Al_2O_3	14.26	12.75	12.00	11.89
Fe_2O_3	0.07	0.15	0.0	0.02
MgO	0.88	1.18	.62	0.47
CaO	4.08	1.44	4.46	1.07
SrO	--	0.32	0.21	--
BaO	2.84	0.83	0.35	--
Na_2O	0.76	3.27	0.45	2.96
K_2O	1.37	0.65	1.36	3.47
Total**	(84.58)	(85.17)	(84.50)	(89.81)
Cell contents based on 72 oxygens				
Si	28.16	29.20	29.53	30.02
Al	7.85	6.80	6.43	6.01
Fe	.02	.06	--	--
Mg	.62	.80	0.42	.30
Ca	2.04	.70	2.17	.49
Sr	--	.08	.06	--
Ba	.52	.15	.07	--
Na	.69	2.87	.39	2.45
K	.82	.37	.79	1.88
$Si+Al+Fe^{3+}$	36.03	36.06	35.96	36.01
Ech	7.85	6.70	6.62	5.91
Error	+0.3%	+1.5%	-3.0%	+1.7%

* From Wise et al. (1969)
** The remainder is the H_2O; the amount is not a good measure of the H_2O content, since some is lost in the vacuum.
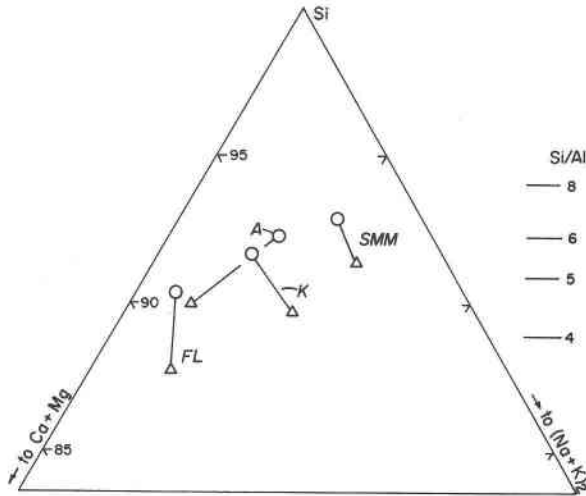
FIG. 4. Si–Ca+Mg–(Na+K₂) plot of associated ferrierite (circles) and clinoptilolite or heulandite (triangles). Locality symbols are the same as in Figure 1. The points represent averages of all analyses of each mineral from each locality.

Summary

The new analyses of ferrierite fill in gaps in a wide range of compositions. This range demonstrates that ferrierite can crystallize from solutions with a wide variety of alkali and alkaline earth cations, none of which are essential to the zeolite. However, Mg ions, if present, are fractionated into ferrierite relative to other zeolites.

Ferrierite crystallizes in response to high silica activities, but the range must be narrow because of the close association with other high silica zeolites. The a_{SiO_2} must be coupled with other variables, such as temperature and/or a_{H_2O}, in order to achieve the range of Si contents observed.

References

ALIETTI, A. E., E. PASSAGLIA, AND G. SCAINI (1967) A new occurrence of ferrierite. *Am. Mineral.* **52,** 1562–1563.

COCKFIELD, W. E. (1947) Geology and mineral deposits of Nicola Map-area, British Columbia. *Geol. Surv. Can. Mem.* **249.**

GRAHAM, R. P. D. (1918) On ferrierite, a new zeolite mineral from British Columbia; with some notes on some other Canadian minerals. *Proc. Trans. Roy. Soc. Can. 3rd Ses., Sect.* **IV,** 185–190.

JONES, A. G. (1959) Vernon Map-area, British Columbia. *Geol. Surv. Can. Mem.* **296.**

MERKLE, A. B., AND M. SLAUGHTER (1968) Determination and refinement of the structure of heulandite. *Am. Mineral.* **53,** 1120–1138.

PASSAGLIA, E. (1970) The crystal chemistry of chabazites. *Am. Mineral.* **55,** 1278–1301.

REGIS, A. J. (1970) Occurrences of ferrierite in altered pyroclastics in central Nevada. *Geol. Soc. Am. Abstr. Programs,* **2,** no. 7, 661.

VAUGHAN, P. A. (1966) The crystal structure of the zeolite ferrierite. *Acta Crystallogr.* **21,** 983–990.

WISE, W. S., W. J. NOKLEBERG, AND M. KOKINOS (1969) Clinoptilolite and ferrierite from Agoura, California. *Am. Mineral,* **54,** 887–895.

YAJIMA, S., T. NAKAMURA, AND E. ISHII (1971) New occurrence of ferrierite. *Mineral. J.* **6,** 343–364.

ZIRKL, E. J. (1973) Ferrierit im Basalt von Weitendorf, Steiermark (Austria). *Neues Jahrb. Mineral. Monatsh.* **11,** 524–528.